TM-1346
2750.000

TEST RESULTS AND DESIGN DETAILS OF THE TOHOKU BUBBLE CHAMBER MAGNET*

W. Craddock and C. Grozis
Fermi National Accelerator Laboratory, Batavia, Illinois

M. Mruzek
KMS Fusion, Ann Arbor, Michigan

September 1985

*Presented at the 1985 Cryogenic Engineering Conference and International Cryogenic Materials Conference, Massachusetts Institute of Technology, Cambridge, Massachusetts, August 12-16, 1985.

TEST RESULTS AND DESIGN DETAILS OF THE TOHOKU BUBBLE CHAMBER MAGNET

W. Craddock and C. Grozis

Fermi National Accelerator Laboratory
Batavia, Illinois

M. Mruzek

KMS Fusion
Ann Arbor, Michigan

ABSTRACT

Fermilab has successfully tested an iron bound 3 Tesla superconducting solenoid for the Tohoku Bubble Chamber. Thermal performance, magnetic fields, charging characteristics, and a special Ni30%Fe dump resistor are reported. Low heat leak is obtained by thermally intercepting the supports with boiloff gas.

INTRODUCTION

A superconducting split solenoid for Fermilab's holographic freon Tohoku Bubble Chamber has been built and successfully tested to its design current. This magnet was originally intended for the 30-inch Bubble Chamber as part of an energy conservation program, but the iron and vacuum shell were modified during construction to accommodate the new larger chamber.

DESIGN AND CONSTRUCTION

The iron bound magnet is layer wound with a solder filled cable on periodic G-10 spacers which provide electrical insulation and cooling channels. Two vertical, gravity feed pool boiling coils have independent cryogenic/vacuum systems which can be moved apart cold with their iron halves for quick maintenance of the chamber. The support system consists of 8 axial and 4 horizontal fiberglass compression posts, 16 Inconel 718 axial preload rods, and 2 vertical stainless steel tension links. Each support has a LN_2 and a helium boiloff gas intercept. Table 1 lists the most important parameters. See reference 1 for further construction and assembly details. Figure 1 is an overall isometric of one half of the system, and Fig. 2 shows a coil cross section through one of the fiberglass epoxy supports. The vacuum shell is five sided to provide clearance to the close fitting bubble chamber.

As part of Fermilab's increasingly tight safety standards and review procedures, extensive finite element analysis was performed using ANSYS

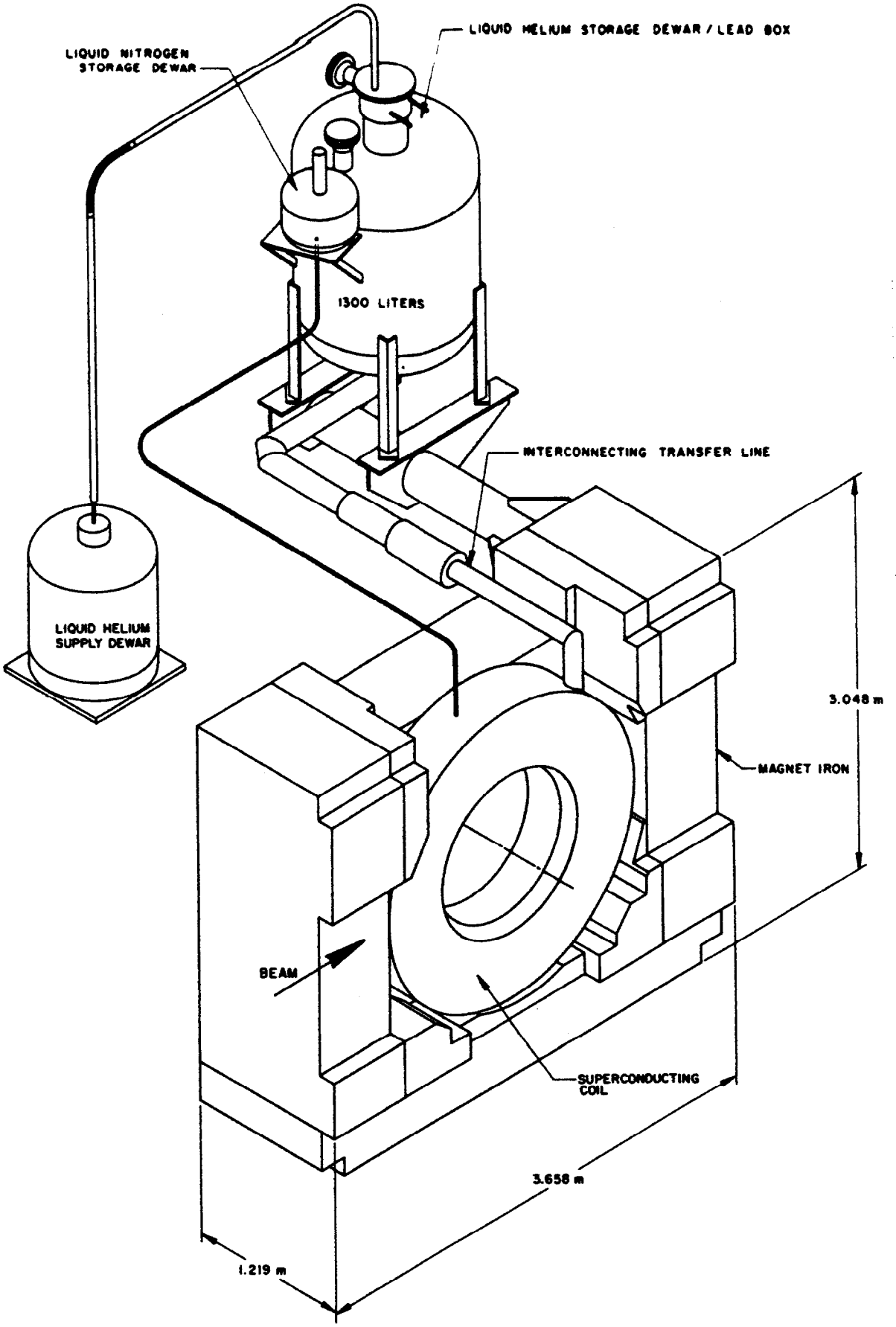

Fig. 1. One half the magnet system.

Table 1. Magnet Parameters

Configuration:	Split solenoid with horizontal axis
Central field:	2.87 T
Clear Bore:	1.15 m (45.23 in.)
Stored Energy:	11.3 MJ
Amp Turns:	1.99×10^6 per coil
Operating Current:	700 amps
Inductance:	46 H
Winding I.D.:	1.28 m (50.3 in.)
Winding O.D.:	1.69 m (66.5 in.)
Maximum Field on Conductor:	5.38 T
Overall Conductor Dimension:	0.231 cm x 0.465 cm = 0.107 cm^2
Conductor Current Density:	8090 amps/cm^2 (based on true area)
Coil Current Density:	4380 amps/cm^2
% Short Sample:	56
Conductor Heat Flux:	0.40 watt/cm^2
Number of Layers:	63
Copper/NbTi:	8.5 layers 1-26 10.1 layers 27-63
Fraction Short Sample:	56%
Conductor Heat Flux:	40 watt/cm^2
Max. Axial Force per Coil (Calculated:	1.1×10^6 Newtons (2.4×10^5 lbf)
Axial Magnetic Spring Constant:	3.5×10^7 Newtons/meter (2.0×10^5 lbf/in.)
Vertical Radial Decentering Force (Measured):	4.0×10^4 Newtons (9100 lbf)
Horizontal Radial Decentering Force (Measured):	1.25×10^5 Newtons (2.8×10^4 lbf)
Measured Helium Boiloff at 700 A:	18 liters/hr
Dump Resistor:	0.85 Ω @ 20°C
Weight of Magnet Iron:	150 metric tons

for all major components of the magnet system. Results show design stress level compliance to Section VIII, Division 2 of the ASME Pressure Vessel Code when 4.2 K material properties were chosen. Cryostats, LHe dewars, LN_2 dewars, and the common vacuum spaces were all pneumatically pressure tested to at least 1.25 times the maximum possible pressure. Computer analysis shows 0.6 MPa is the maximum possible pressure in the helium system. In the event of a massive quench, the 80 liters of helium in the cryostat would be rapidly expelled up into the storage dewar resulting in a supercritical or a compressed liquid state. Coil winding would then absorb all remaining heat. Emergency vent lines are installed on only the LHe system. Helium boiloff gas is normally recovered by the 15 Foot Bubble Chamber Magnet.

MAGNET COOLDOWN AND THERMAL PERFORMANCE

A LN_2 precool was started on March 18, 1985. Accumulated LN_2 was blown out by pressurization with the remaining traces removed by a vacuum pump. LHe cooldown as well as the LN_2 cooldown both use the flexible liquid helium transfer line shown in Fig. 1. Due to its unweildy 12 meter length, this line remains in the storage dewar at all times. For cooldown the liquid helium transfer line is seated in a polished cone at the bottom of the storage dewar. This is connected to a small line running to the very bottom of the magnet for efficient cooling. At all other times the transfer line is unseated to gravity feed LHe to the coil. Figure 3 shows this line and the overall helium boiloff cooling scheme.

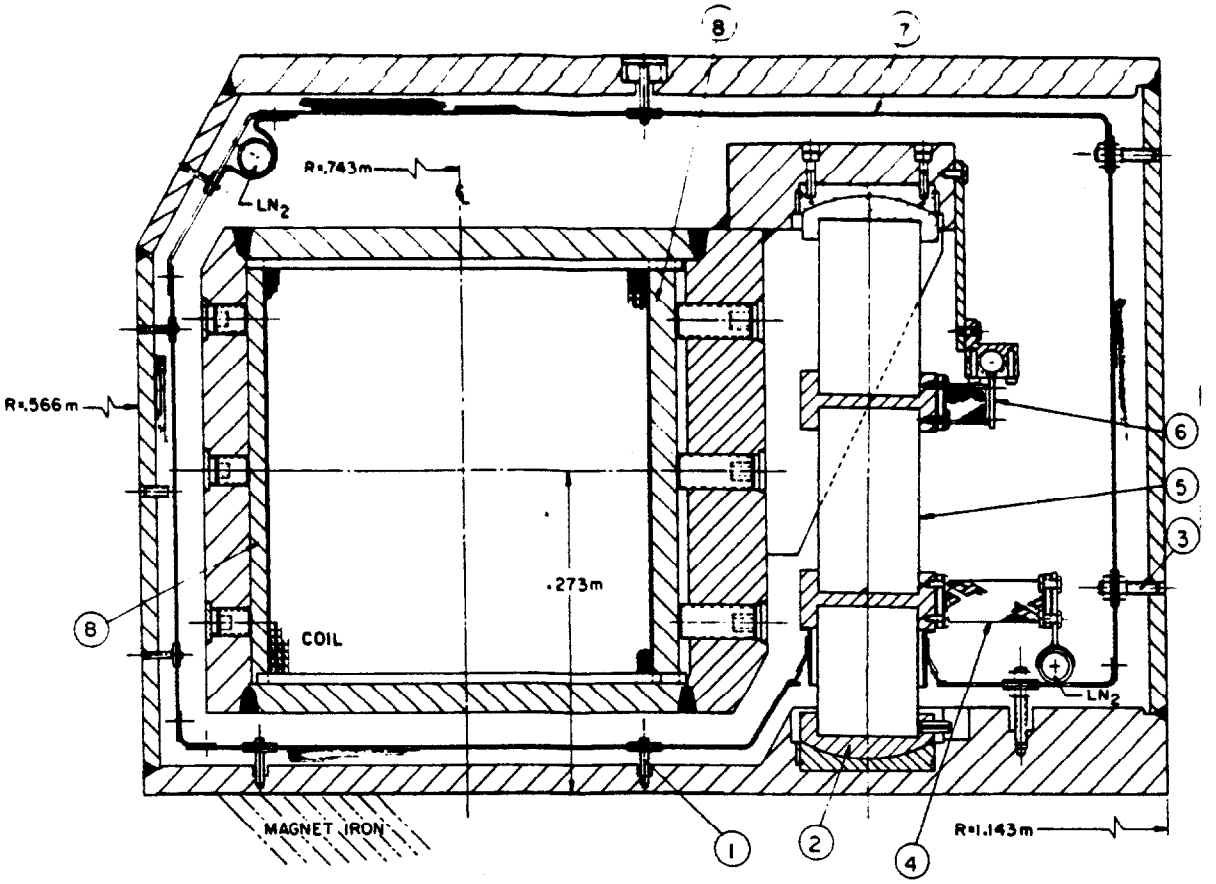

Fig. 2. Coil cross section through an axial support post. LEGEND: (1) Ti6Al4V standoff; (2) 7075-T6 aluminum spherical bearing surface; (3) G-10 standoff; (4) copper braid; (5) Randolite fiberglass epoxy axial support; (6) ∿10 K He gas intercept; (7) LN_2 shield; (8) coil preload bars.

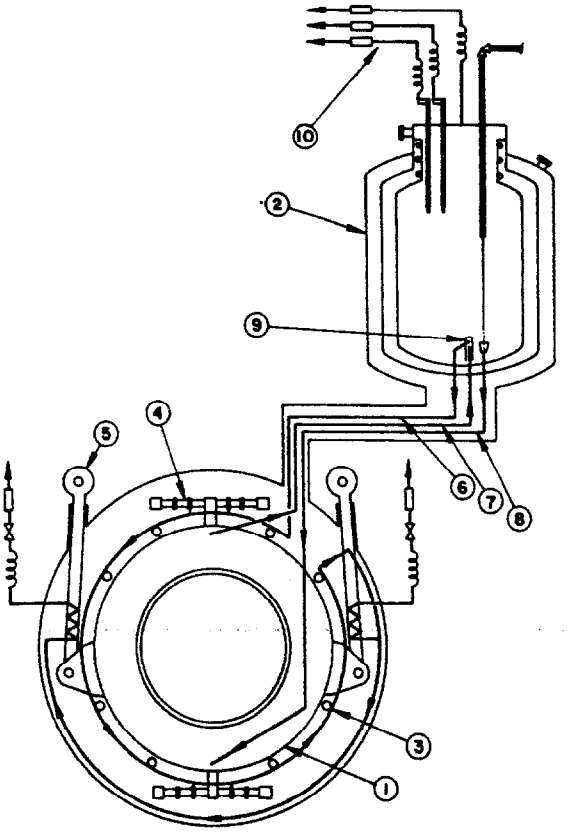

Fig. 3. Helium flow schematic for one coil. LEGEND: (1) coil; (2) LHe storage dewar; (3) fiberglass epoxy axial support; not shown are two small Inconel 718 preload rods; (4) fiberglass horizontal support; (5) vertical tension links; (6) helium boiloff gas to supports; (8) LHe cooldown line and normal supply line; (9) gas collection can; (10) helium cooling vent lines for current leads and dewar neck.

The support system is designed to carry 2.2×10^6 N axial, 7.8×10^5 N vertical, and 3.3×10^5 N horizontal loads. As shown in Fig. 3, vaporized helium from the coil is collected in the dewar and routed back to the 12 fiberglass supports in an internally finned tube. Thermal connections are made with a copper braid. After intercepting the last post, the gas stream is split between the two stainless steel vertical supports. The helium flows up each member in a serpentine fashion through a series of 38 holes which have been threaded for improved heat transfer. Large forces and little available room for support members necessitated using this complex cooling scheme.

Within construction constraints all helium intercepts for axial/horizontal supports are placed at their optimum location. An energy balance for self-sufficient mass flow gives the following results[2].

$$\gamma = Q_1/Q_0 = \frac{1 + C\,(T - 4.2)\,B}{1 + C\,(T - 4.2)} = \frac{\text{heat from a self-sufficient cooled support}}{\text{heat from an uncooled support}}$$

$$\ell_1/L = \frac{\ell_1}{\ell_1+\ell_2} = B/\gamma$$

where

$$Q_1 = \frac{A}{\ell_1}\int_{4.2}^{T} K(T)dT \quad ; \quad Q_2 = \frac{A}{\ell_2}\int_{T}^{T_{LN2}} K(T)dt \quad ; \quad Q_0 = \frac{A}{L}\int_{4.2}^{T_{LN2}} K(T)dt$$

ℓ_1 = length between 4.2 and the intercept at temperature T

ℓ_2 = length between T and the LN_2 intercept at temperature T_{LN2}

A = area of the support

$C = C_p/\Delta h_v$

$$B = \int_{4.2}^{T} K(T)dT \;\Big/\; \int_{4.2}^{T_{LN2}} K(T)dT$$

To find the optimum location and heat leak, plot γ and ℓ_1/L versus T. With a self-sufficient flow these supports have a heat leak of 1.15 watts per coil which is only 22% of an uncooled system. Heat leak other than for self-sufficient mass flow can also be calculated with an energy balance. When the boiloff gas from other heat sources is added to the intercept stream there is an overall reduction in the heat load. For external heat loads up to the size of the self-sufficient support heat load, -0.55 watts are generated per watt of external heat. Any metallic or nonmetalic support optimized near the self-sufficient point should have similar performance.

Both the vertical tension links and the dewar neck are cooled in a continuous fashion with boiloff gas[3]. The self-sufficient heat leak for these supports is 1.16 watts per coil, only 9% the heat leak of the uncooled case. A minimum 4.2 K heat load of 0.56 watts is found due to the finite distance between 4.2 K and the start of the 15 K gas leaving the axial/horizontal supports.

Totaling all heat loads at 700 Amps for the entire magnet gives:

14 watts = 20 liter/hr (4.2 K, all supports self sufficient)

10 watts = 14 liter/hr (4.2 K, theoretical minimum)

13 watts = 18 liter/hr (4.2 K, measured heat leak based on liquid level rather than generated gas)

52 watts = 74 liter/hr (4.2 K, no gas cooling)

790 watts = 18 liter/hr (calculated LN_2 heat load)

1030 watts = 23 liter/hr (measured LN_2 boiloff rate)

Two pair of current leads contribute 4.2 watts or 1/3 of the 4.2 K heat load. LN_2 intercepts were measured at 100 K with the remainder of the LN_2 shield at 90 K. A thermal syphon technique relying on bouancy difference circulates the LN_2. The small dewar in Fig. 1 feeds LN_2 to the bottom of the magnet in an insulated line. The return pipe back to the dewar intercepts all the supports and radiation including those in the LHe dewar shield. There is no easy method to measure this flow rate.

MAGNETIC FIELD CALCULATIONS AND TEST RESULTS

The magnetic field was calculated with cylindrical symmetry using TRIM. Compare the iron model in the Fig. 4 flux plot with the actual iron shape in Fig. 1. Magnetic fields, axial forces, and decentering forces were all measured. At full current, 700 Amps, the measured central field of 2.89 T is only 1% greater than the calculated value. Magnetic forces are listed in Table 1. Reliable measured axial forces are not available due to instrumentation problems, although both measured and calculated axial force maximums occur very near 600 Amps. Vertical forces are much smaller than the design value since large air gaps for muons were machined off the bottom of the iron for the new experiment. Both downstream vertical supports have six times the load of the upstream supports. Lack of iron symmetry across the vertical midplane is the most probable cause.

The magnet was tested to full current on April 16, 1985 by successively ramping and discharging in increasing ~100 Amp increments.

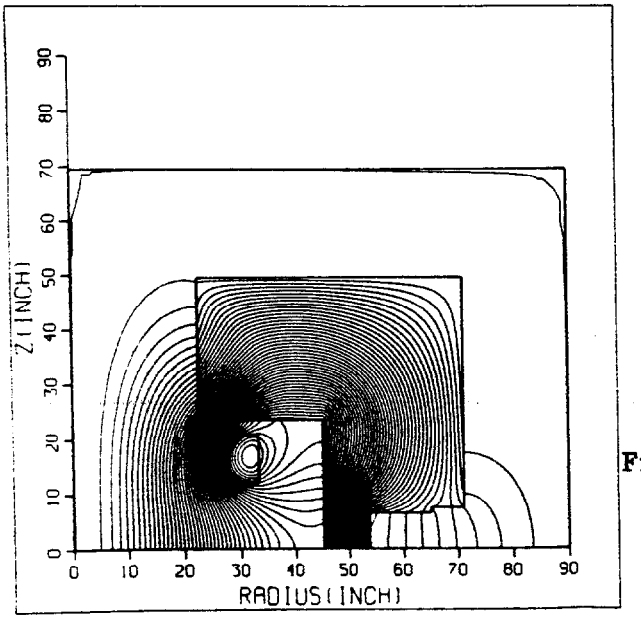

Fig. 4. TRIM magnetic flux line plot. Air gap areas and distances at the midplane of this model equal the air gaps shown in Fig. 1.

Voltage imbalance between the coils which functions as the quench detector was continuously recorded during testing. A condensed voltage imbalance history shown in Fig. 5 clearly shows larger voltage spikes as a function of higher current. This curve is a composite of typical signals seen in each 50 Amp increment. Total charge time is 32 minutes. Voltage spikes correspond to small transients created as the windings shift. In the 300 to 600 Amp range audible "pinging" was clearly heard simultaneously with the voltage spikes. A 64 mV peak was the largest recorded. The Chicago Cyclotron Magnet was built with identical cable and had similar electrical behavior except that its largest voltage spikes were on the order of several volts[4]. The Tohoku Bubble Chamber Magnet is thought to have much greater radial preload and tighter coil package; therefore, smaller conductor motions should be possible.

From 600 to 700 Amps very little acoustical and electrical noise were present. Interestingly, 600 Amps corresponds to exactly the peak in the axial force. Radial compression of these windings were excellent, but axial preload was done by hand with small shims and is far from perfect. The conductors were bonded to the interlayer spacers with epoxy. One can conclude voltage spikes caused by axial conductor motion would be present in any magnet of similar construction.

On subsequent ramps virtually no voltage spikes are present except those induced by the pulsing of the chamber which are on the order of 15 mV. Inductance between the two halves is matched very precisely, and only a 20 mV imbalance shift occurs between 0 and 700 Amps. If iron and coils halves were not nearly identical, our 50 mV quench trip level would have been difficult to achieve.

Magnet stability is maintained by operating below the cold end recovery current. No quenches have occurred, but the energy could be safely removed during a quench with the dump resistor used for normal discharge. This resistor is specially designed with a 70% Ni 30% Fe alloy having a large coefficient of resistivity. Instead of an exponential decay, the resistor/magnet combination roughly approximates a constant voltage decay. Using this technique permits a lower maximum discharge voltage for a given maximum adiabatic hot spot temperature calculated from

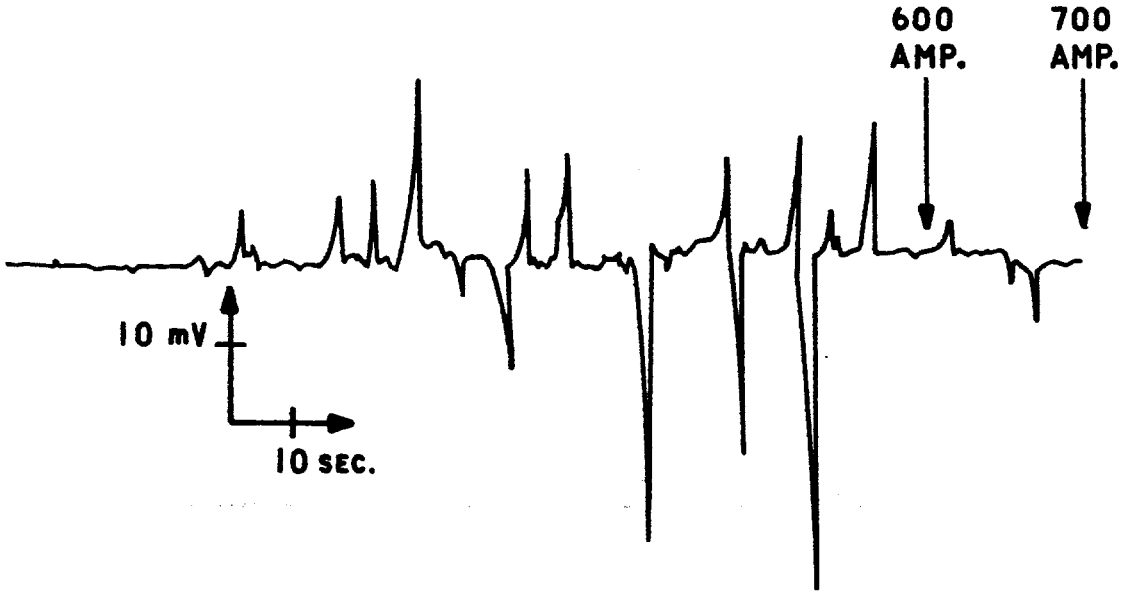

Fig. 5. A condensed voltage record during the first charge to 700 Amps. For each 50 Amp increment a typical signal was selected.

$$\int_0^{\infty} I^2 dt = \int_{293}^{T} \frac{C_p(T)}{R(T)}\, dt$$

At 710 Amps the hot spot temperature is calculated to be 265 K. A 650 Volt maximum appears ~10 seconds into the discharge. If a resistor with constant value were used, a 900 Volt discharge would have been necessary for the same limiting conductor temperature. A perfect constant voltage discharge has only 2/3 the peak voltage of an exponential discharge. Our magnet/resistor comes close to this theoretical limit.

REFERENCES

1. W. Craddock et al, Coil Conversion of the Fermilab 30-Inch Bubble Chamber Magnet, in: "Advances in Cryogenic Engineering", Vol. 27, Plenum Press, New York (1982), p. 119.

2. I. Pless and T. Stoughton, "FHS Magnet Technical Memo No. 1", Private Communication, (1979).

3. R. B. Scott, "Cryogenic Engineering", Van Nostrand, Princeton, N.J., (1967), p. 239.

4. E. Leung et al, The Superconducting Chicago Cyclotron Magnet, in, "Advances in Cryogenic Engineering," Vol. 27, Plenum Press, New York (1982), p. 135.